Learning Intention Aware Online Adaptation of Movement Primitives

Dorothea Koert, Joni Pajarinen, Albert Schotschneider, Susanne Trick, Constantin Rothkopf, and Jan Peters

***Abstract*—In order to operate close to non-experts, future robots require both an intuitive form of instruction accessible to laymen and the ability to react appropriately to a human co-worker. Instruction by imitation learning with probabilistic movement primitives (ProMPs) allows capturing tasks by learning robot trajectories from demonstrations, including the motion variability. However, appropriate responses to human co-workers during the execution of the learned movements are crucial for fluent task execution, perceived safety, and subjective comfort. To facilitate such appropriate responsive behaviors in human–robot interaction, the robot needs to be able to react to its human workspace co-inhabitant online during the execution of the ProMPs. Thus, we learn a goal-based intention prediction model from human motions. Using this probabilistic model, we introduce intention-aware online adaptation to ProMPs. We compare two different novel approaches: First, online spatial deformation, which avoids collisions by changing the shape of the ProMP trajectories dynamically during execution while staying close to the demonstrated motions and second, online temporal scaling, which adapts the velocity profile of a ProMP to avoid time-dependent collisions. We evaluate both approaches in experiments with non-expert users. The subjects reported a higher level of perceived safety and felt less disturbed during intention aware adaptation, in particular during spatial deformation, compared to non-adaptive behavior of the robot.**

***Index Terms*—Human-centered robotics, learning and adaptive systems, human factors and human-in-the-loop.**

Manuscript received February 20, 2019; accepted June 25, 2019. Date of publication July 15, 2019; date of current version July 26, 2019. This letter was recommended for publication by Associate Editor I. Nisky and Editor A. M. Okamura upon evaluation of the reviewers' comments. This work was supported in part by the German Federal Ministry of Education and Research (BMBF) project 16SV7984, in part by the ERC StG 640554, and in part by the German Research Foundation project PA 3179/1-1. *(Corresponding author: Dorothea Koert.)*

D. Koert is with the Intelligent Autonomous Systems and the Centre for Cognitive Science, TU Darmstadt, 64289 Darmstadt, Germany (e-mail: koert@ias.tu-darmstadt.de).

J. Pajarinen is with the Intelligent Autonomous Systems, TU Darmstadt, 64289 Darmstadt, Germany, and also with the Tampere University, FI-33014 Tampere, Finland (e-mail: pajarinen@ias.tu-darmstadt.de).

A. Schotschneider is with the Intelligent Autonomous Systems, TU Darmstadt, 64289 Darmstadt, Germany (e-mail: albert.schotschneider@stud.tu-darmstadt.de).

S. Trick is with the Centre for Cognitive Science and the Psychology of Information Processing, TU Darmstadt, 64289 Darmstadt, Germany (e-mail: susanne.trick@cogsci.tu-darmstadt.de).

C. Rothkopf is with the Centre for Cognitive Science and the Psychology of Information Processing, TU Darmstadt, 64289 Darmstadt, Germany, and also with the Frankfurt Institute for Advanced Studies, Goethe University, 60323 Frankfurt, Germany (e-mail: rothkopf@fias.uni-frankfurt.de).

J. Peters is with the Intelligent Autonomous Systems and the Centre for Cognitive Science, TU Darmstadt, 64289 Darmstadt, Germany, and also with the MPI for Intelligent Systems, 72076 Tuebingen, Germany (e-mail: peters@ias.tu-darmstadt.de).

This letter has supplementary downloadable material available at http://ieeexplore.ieee.org, provided by the authors. The material consists of a video, viewable with mp4 format and can be played with a standard media player, e.g., VLC media player, In this video, "Learning Intention Aware Online Adaptation of Movement Primitives." The size of the video is 8.36 MB. Contact: Dorothea Koert (koert@ias.tu-darmstadt.de) for further questions about this letter.

Digital Object Identifier 10.1109/LRA.2019.2928760

I. Introduction

In CONTRAST to classical robotic domains, where robots usually operate at a safe distance from humans, future robot applications such as elderly assistance or interactive manufacturing aim to bring robots closer to everyday contact with humans [1]. In this context learning from demonstration [2] and the concept of movement primitives [3]–[5] offer a promising approach for non-expert users to teach new tasks to robots. In particular, probabilistic movement primitives (ProMPs) [5] can capture the inherent variability in the demonstrated motions. However, when a robot is supposed to share a workspace in close proximity with a human, special requirements for online adaptation of learned robot motions arise. While ProMPs have been already extended for collaborative tasks [6] and offline planning methods with static obstacles [7], [8] exist, to the best of the authors' knowledge no method for online human aware adaptation of ProMPs in shared workspaces has been introduced so far. Such an approach needs to be able to react online to dynamic changes in human intentions and motion goals. To avoid extensive replanning and the resulting inconsistency of robot motions, it is desirable to predict behavior changes of humans in advance. As human behavior might differ between situations and subjects it is desirable to learn both movement goals and motion behavior of humans from observations and in an online manner. Such motion models can predict potential collisions between the human and the robot in advance and adapt the robot's movements accordingly.

The contribution of this letter are two novel approaches for intention aware online adaptation of ProMPs and their evaluation with non-expert users.

The two approaches are inspired by time-dependent human collision avoidance behaviors, namely change in path direction and change in path velocity as also observed e.g., in pedestrian motions [9], [10]. Our first approach optimizes the shape of the ProMP for spatial obstacle avoidance, taking into account information from the demonstrations, and follows a similar approach as [8]. However, while [8] only proposed offline optimization our approach runs online and is able to react to dynamically changing human motions. The second novel approach optimizes the velocity profile of the ProMP to achieve obstacle avoidance while the motion path remains unchanged. For predicting human motions, both of the new online ProMP adaptation techniques

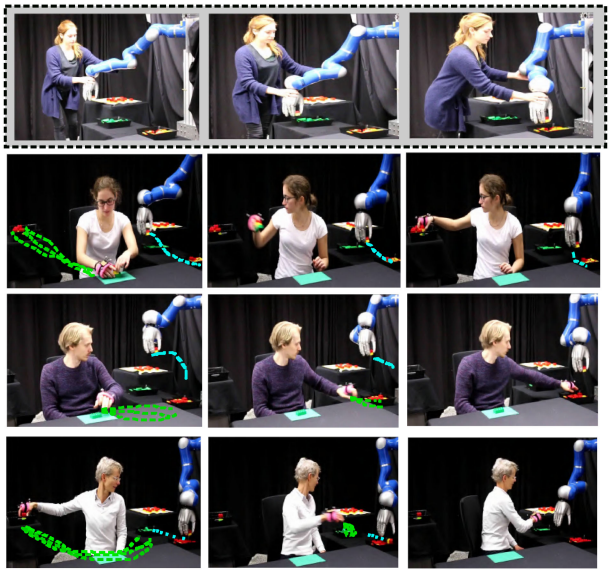

Fig. 1. We learn probabilistic movement primitives for a pick-and place task via kinesthetic teaching (upper row). When executed in a shared human robot workspace as shown in row 2-4 the learned motions need to be adapted online. To this end, we propose a novel approach for human aware execution of ProMPs by incorporating goal directed predictions of human motions (green) with two novel approaches for online adaptation of ProMPs, namely spatial deformation (third row) and temporal scaling (last row). We compare those two approaches to non reactive ProMP execution (second row).

use a goal-directed probabilistic prediction model learned from observations.

Commonly in pure motion planning the reaction of a human to the robot's motions is not the focus of investigations as long as collisions with the human are avoided. However, in human aware motion adaptation human presence gives need to also investigate how different types of robot motions influence a human working in the same workspace [11]–[13]. Therefore, we conducted a user study with non-experts to evaluate the effects of our spatial and temporal motion adaptation approach on human task performance and subjectively perceived levels of comfort, safety and predictability of the robot's motions.

The rest of the letter is structured as follows: Section II, presents related work. Section III summarizes the concept of ProMPs and introduces our novel approaches for online adaptation of ProMPs to dynamic obstacles and a probabilistic model for predicting goal directed human motions. Section IV presents results from a user study where we evaluated both online adaptation approaches and the prediction model on a pick and place task. In Section V, we draw conclusions from the experiments and discuss possible future work.

II. Related Work

Efficient and safe coexistence of robots and humans has been a longstanding robotics challenge [14], [15]. In particular, when a human is in close proximity to the robot the situation differs from classical motion planning due to the human being highly dynamic and possibly reacting subjectively to different ways the robot moves [11], [13], [16]. While earlier approaches to human robot collaboration often consider safety zones or velocity limits [14], [17] more recent research investigates ways to generate human aware robot motions in close proximity and shared workspaces [18]–[22]. Mainprice et al. proposed a Gaussian Mixture Model (GMM) for predicting human motions and used constrained stochastic trajectory optimization to spatially deform robot trajectories [18], [23].

Additionally, approaches for online trajectory deformation based on physical input signals from a human [20], human comfort and ergonomic postures [21], or optimizing human robot handovers have been presented [22], [24]. These approaches mainly focus on deformation of trajectories. Adapting the motion speed has been used in human-robot interaction to decrease potential impact force [15], slow down the robot when a human enters a monitored area [17], for online obstacle avoidance of two robots in a cooperative setting [25], and for time-dependent collision avoidance in navigation tasks with mobile robots [26]–[28].

For more efficient human robot co-working or collaboration and to avoid the need for extensive replanning, early prediction of human intentions is crucial. In particular, predicting human motion goals and reaching motions has been exploited in the literature [26], [29], [30]. Recently, also Gaussian Mixture models [31] or probabilistic movement primitives [32] have been used for early intention prediction of human motions. In collaborative assembly, [33] controls the velocity of a robotic system along a linear axis dependent on potential collisions with co-workers.

Recent studies with non-expert users report the benefits of such human aware planning approaches for mobile robots [27], [28] and in shared workspaces with robot manipulators [11]. They also report the contrast between legibility and predictability in motions [13] and effects of motion speed and predictability [16]. However, non-expert user studies on different online replanning behaviors are rare in the literature, but important to better understand human responses to robot motions.

Contrary to many of the previously mentioned methods, our approach incorporates movement primitives which we will discuss in the following. Movement primitives [3]–[5] provide a lower dimensional representation of trajectories and an intuitive way for non-experts to teach new tasks to a robot by demonstrations. In particular, Probabilistic Movement primitives offer a framework to capture the inherent variability of the motions [5].

For dynamic movement primitives the use of repellent forces was proposed for obstacle avoidance [34], [35], and for dynamic systems approaches the use of potential fields is presented in [36]. Saverino proposes human-aware motion reshaping using dynamical systems [37], where the robot adapts velocity and its motion goal online dependent on human motion. In particular, they also introduce a RGBD camera based approach for fast and efficient distance computation to the human. However, they do not incorporate prediction models for human motions and do not conduct user studies on perceived subjective safety or comfort.

ProMPs have been extended to collaborative tasks [6] and offline trajectory planning [7]. However, the computationally expensive sample based Kullback-Leibler Divergence in [7] prevents online replanning. Colome et al. [8] proposed a demonstration free version of ProMPs and use the Mahalanobis distance to the demonstrations for static obstacle avoidance without online replanning. However, in a setting with a human present, dynamic obstacle avoidance, which is capable of human aware online replanning, is crucial.

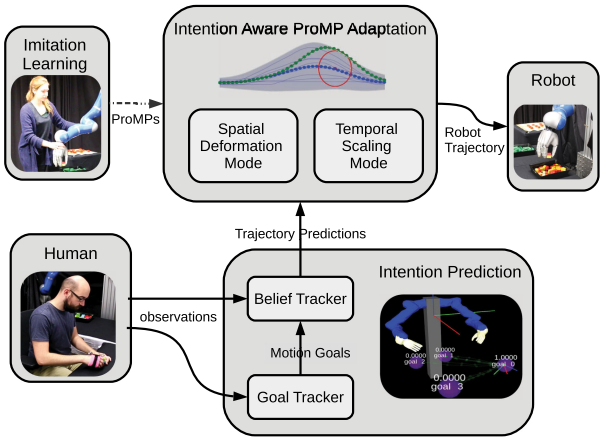

Fig. 2. We propose two novel approaches for online human aware adaptation of ProMPs, namely spatial deformation and temporal scaling. Therefore we learn a goal-directed probabilistic prediction model from observing human motions and use predictions from this model to online adapt ProMPs, which are originally learned via imitation learning.

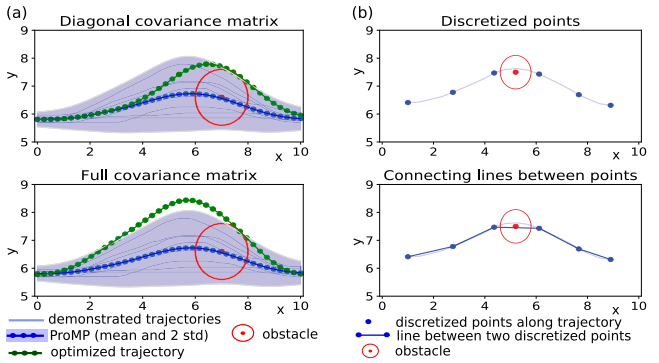

Fig. 3. (a) When only the diagonal of the covariance is used for optimization the trajectory stays closer to the ProMP's mean in regions unaffected by the obstacle. When using the full covariance matrix, the optimized trajectory will stay closer to the correlation of the demonstrations. (b) It is advantageous to not only compute obstacle distances for discretized points but of connections between points to enable a more sparse discretization.

III. Intention Aware Online ProMP Adaptation

We propose two novel approaches for online intention aware adaptation of ProMPs, namely spatial deformation and temporal scaling. In both cases, we first learn a goal-directed motion model from observations of human task execution and use this probabilistic prediction model to online adapt ProMP trajectories afterwards. For spatial deformation, we online deform the current path of the robot to avoid dynamic obstacles while staying close to demonstrated distributions. For temporal scaling, we solely adapt the velocity profile of the ProMP while staying on the original path. Figure 2 illustrates the different components of our approach.

We first recap on ProMPs and then present our two approaches for online adaptation of ProMPs to dynamic obstacles, namely spatial online deformation and temporal scaling of the ProMP. Moreover, we introduce our probabilistic model for goal-based prediction of human motions.

A. Probabilistic Movement Primitives

Probabilistic Movement Primitives (ProMPs) [5] provide a lower dimensional representation of trajectory distributions. The trajectory distribution is obtained from an approximation of demonstration trajectories by a linear combination of basis functions ϕ. In particular, the representation for a joint or Cartesian position x_t at time step t is given as

$$x_t = \boldsymbol{\phi}(t)^T \boldsymbol{w} + \epsilon, \tag{1}$$

where $\boldsymbol{w}$ is a weight vector, $\boldsymbol{\phi}(t)$ consists of N basis functions ϕ evaluated at time step t, and ϵ is zero-mean Gaussian noise. A common choice for the basis functions are radial basis functions. Here we used 7 radial basis functions per dimension. Using Ridge Regression, one obtains the weight vector $\boldsymbol{w}$ for each demonstrated trajectory.

To account for the variability in the demonstrations a Gaussian distribution over the weight vectors $p(\boldsymbol{w}) = \mathcal{N}(\boldsymbol{\mu_w}, \boldsymbol{\Sigma_w})$ is obtained with Maximum Likelihood estimation. Using a normalized representation of time is common in ProMPs. Hereby, a phase variable z is defined as $z = \alpha t$ with $0 < z < 1$, where t represents time and α a scaling factor that is related to the execution speed of the movement primitive. More details on ProMPs can be found in [5].

B. Online Spatial Deformation of ProMPs

We propose online spatial adaptation of ProMPs by optimizing the current weight vector of the ProMP which results in spatial deformation of the resulting trajectory. To this end, we propose a constrained optimization problem to obtain an updated weight vector $\boldsymbol{w}$ that minimizes the Mahalanobis distance to the original ProMP weight distribution $p(\boldsymbol{w})$ and constrain the minimal distance to obstacles as well as sudden changes in the resulting trajectory

$$\begin{aligned} \arg\min_{\boldsymbol{w}} \quad & (\boldsymbol{w} - \boldsymbol{\mu}_w)^{\mathrm{T}} \mathrm{diag}(\boldsymbol{\Sigma}_{\boldsymbol{w}}^{-1})(\boldsymbol{w} - \boldsymbol{\mu}_w) \\ \text{s.t.} \quad & \varepsilon_{\mathrm{o}} > \Delta(\boldsymbol{\phi}_{t-1}, \boldsymbol{\phi}_t, \boldsymbol{w}, \boldsymbol{O}_t) \quad \forall t, \\ & \varepsilon_{\mathrm{w}} > (\boldsymbol{\phi}_t \boldsymbol{w} - \boldsymbol{\phi}_t \boldsymbol{w}_{\mathrm{curr}})^{\mathrm{T}} (\boldsymbol{\phi}_t \boldsymbol{w} - \boldsymbol{\phi}_t \boldsymbol{w}_{\mathrm{curr}}), \end{aligned} \tag{2}$$

where ε_{o} denotes the bound for the minimal distance to an obstacle, $\boldsymbol{O}_t$ denotes a vector of obstacles at time t, Δ denotes the minimum distance of the discretized robot trajectory to the obstacle vector, which we discuss in more detail later, and ε_{w} limits the change of the weight vector in the current position of the trajectory.

For the Mahalanobis distance, we use the diagonal of the covariance matrix of the weight distribution, as a high correlation between the weights prevents the trajectory from only deforming in regions affected by obstacles. When using the full covariance the optimized trajectory stays closer to the correlations in the demonstrations which may be also desirable in certain applications. However, in our application the optimized trajectory should stay close to the mean in areas unaffected by obstacles. This is also illustrated in Figure 3(a).

Using the Mahalanobis distance to stay close to the demonstrated distribution has also been proposed in [8] for offline trajectory optimization. However, [8] uses it as a constraint while we use it as the objective of the optimization problem. As we run the optimization online, we additionally constrain the possible changes in Cartesian or joint space resulting from

a change in the weight vector to avoid jumps in the trajectory. To compute the closest distance of the resulting trajectory to obstacles, we discretize over time. However, a sparse discretization over time can be problematic as illustrated in Figure 3. Therefore, we compute the minimum distance of the connecting line between two subsequent time steps to the obstacles, as also proposed in [38] for stochastic trajectory optimization. We compute the minimum distance $d_{\min}(\boldsymbol{\phi}_{t-1}, \boldsymbol{\phi}_t, \boldsymbol{w}, \boldsymbol{o})$ to an obstacle $\boldsymbol{o}$ as the minimum distance between the line connecting the two subsequent trajectory points $t-1$ and t and the obstacle:

$$d_{\min}(\boldsymbol{\phi}_t, \boldsymbol{\phi}_{t-1}, \boldsymbol{w}, \boldsymbol{o}) = \frac{|\boldsymbol{v}_1 \times \boldsymbol{v}_2|}{|\boldsymbol{v}_1|},$$
$$\boldsymbol{v}_1 = \boldsymbol{\phi}_t \boldsymbol{w} - \boldsymbol{\phi}_{t-1}\boldsymbol{w}, \qquad \boldsymbol{v}_2 = \boldsymbol{\phi}_{t-1}\boldsymbol{w} - \boldsymbol{o}, \tag{3}$$

where $\times$ denotes the cross product and $|\cdot|$ denotes the Euclidean norm. We compute the minimum over all obstacles at time step t as

$$\Delta(\boldsymbol{\phi}_{t-1}, \boldsymbol{\phi}_t, \boldsymbol{w}, \boldsymbol{O}_t) = \min_{o \in O_t}(d_{\min}(\boldsymbol{\phi}_{t-1}, \boldsymbol{\phi}_t, \boldsymbol{w}, \boldsymbol{o})). \tag{4}$$

This allows for a more sparse discretization which results in more efficient computation. Figure 3(b) illustrates the advantages over computing point-wise distances. To increase efficiency we utilize knowledge from the demonstrations: we initialize the optimization of the spatially deformed trajectory with a demonstrated trajectory that has the maximal distance to the obstacle compared to other demonstrations.

C. Online Temporal Scaling of ProMPs

Instead of modifying the chosen path direction, a common technique for humans to avoid time-dependent collisions with dynamic obstacles is to adapt the velocity along the robot's path [9], [10]. To achieve adaptive online velocity scaling of ProMPs we propose the use of a generalized logistic function $\sigma(\bar{z})$ to compute the phase velocity δz for a given phase z:

$$\sigma(\bar{z}) = \delta z_0 + \frac{\delta z_N - \delta z_0}{1 + (1/\varepsilon_{\text{start}})\exp(m(\bar{z}_{\text{c}} - \bar{z}))}, \tag{5}$$

where $\bar{z}$ is the phase scaled to [0, 100] this is $\bar{z} = 100z$, δz_0 is the starting phase velocity, δz_N is the resulting end velocity, m controls the slope of the velocity change and $\bar{z}_{\text{c}}$ denotes the phase where the velocity change starts, which is the point when the resulting $\sigma(\bar{z}_{\text{c}})$ deviates by a predefined small value $\varepsilon_{\text{start}}$ from δz_0. This function can encode smooth deceleration and acceleration profiles depending on the chosen parameter values as illustrated in Figure 4. The phase velocity δz is then computed as

$$\delta z = \delta z_{\max} \sigma(\bar{z}), \tag{6}$$

where $\delta z_{\max}$ denotes the upper limit for the phase velocity. Once we detect potential collisions with obstacles along the path we compute the phase of collision $\bar{z}_{\text{stop}}$ with an obstacle from a discretized phase vector and subsequently adapt the parameters of the generalized logistic function for a deceleration dependent on the slowing down phase duration

$$\gamma = \bar{z}_{\text{stop}} - \bar{z}_{\text{c}}, \tag{7}$$

where $\bar{z}_{\text{stop}}$ is the point in time where the phase velocity decreases below a predefined small value $\varepsilon_{\text{stop}}$, resulting in the robot stopping. Here we used $\varepsilon_{\text{stop}} = \varepsilon_{\text{start}} = 0.1$. For a given

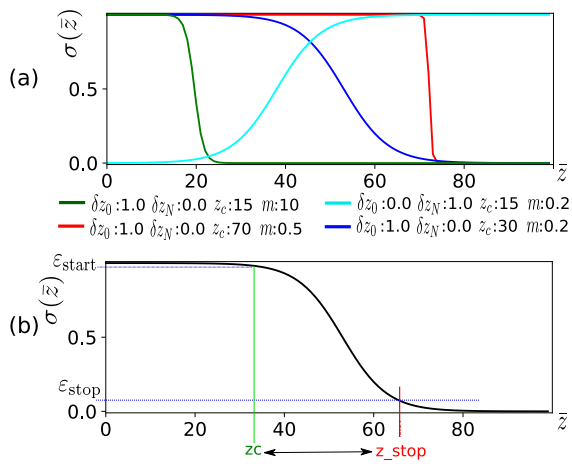

Fig. 4. (a) Depending on the choice of the parameters the generalized sigmoid function results in smooth slowing down (dark blue), rapid stopping (green) or accelerating behavior (light blue) along the path. (b) For a given desired stop phase z_{stop} and a given optimal deceleration duration we can compute the parameters of the resulting deceleration profile.

$\bar{z}_{\text{stop}}$ and the current phase $\bar{z}_n$ we can compute γ by solving the constrained optimization problem

$$\arg\min_{\gamma}(\gamma - \gamma_{opt})^2, \quad \text{s.t.} \quad \bar{z}_{\text{stop}} - \gamma > \bar{z}_n, \tag{8}$$

where γ_{opt} denotes a desired optimal slowing down duration, that needs to be chosen a priori. Given the optimized γ^* we can compute from Equation (7) the phase where the velocity change starts $\bar{z}_c^* = \bar{z}_{\text{stop}} - \gamma^*$. Next, we compute the slope m^* by solving Equation (5) for m, plugging in the knowledge we already have about the slowing down parameters

$$\sigma(\bar{z}_{\text{stop}}) = \varepsilon_{\text{stop}}, \quad \delta z_0 = 1 \quad \delta z_N = 0 \tag{9}$$

$$m^* = \log\left(\frac{\varepsilon_{\text{stop}}\varepsilon_{\text{start}}}{1 - \varepsilon_{\text{stop}}}\right) \Big/ (-\gamma^*), \tag{10}$$

and use m^* and $\bar{z}_c^*$ to update the velocity profile. This results in a smooth slowing down of the ProMP if an obstacle is predicted in advance to be on the path and in a hard stop if the obstacle crosses the path unexpectedly. Once the robot has no potential collisions along the path anymore, we adapt the sigmoid function to accelerate again to the original speed.

D. Probabilistic Model for Human Trajectory Prediction

To avoid the need for extensive online replanning and to ensure consistency in the robot motions we additionally propose a probabilistic model for human intention and trajectory prediction. This model can run online and learns human motion goals and transition probabilities between them from observations. The model consists of a goal tracker, which extracts human motion goals from observations using an incremental Gaussian Mixture model and a belief tracker that computes probabilities of currently active goals and transitions between them from a history of previous observations.

1) Goal Tracker: We propose an online and open ended approach to learn a distribution over possible Cartesian movement goal positions from human wrist trajectories. Hereby, a goal tracker extracts potential motion goals $\boldsymbol{g}$ from human motion data by learning a Gaussian Mixture model (GMM) over zero

velocity points $\boldsymbol{p}_i$. The distribution $p(\boldsymbol{g})$ over goals $\boldsymbol{g}$ is represented as

$$p(\boldsymbol{g}) = \sum_{k=1}^{K} \alpha_k \, \mathcal{N}\big(\boldsymbol{g} \,|\, \boldsymbol{\mu}_k^g, \boldsymbol{\Sigma}_k^g\big) \tag{11}$$

where α_k denotes the prior, K denotes the total number of goals, $\boldsymbol{\mu}_k^g$ is the mean and $\boldsymbol{\Sigma}_k^g$ is the covariance of the k-th component respectively. We assume uninformed priors in our model such that $\alpha_k = 1/K$.

In an online setting, the total number of motion goals is not known a priori. Therefore, we propose to learn the model incrementally using an incremental Gaussian Mixture model [39]. Hereby, we first extract potential goal points $\boldsymbol{p}_i$ from observations of the human wrist position. The potential goal points are zero velocity points that are points where the change in wrist position stays below a predefined threshold for a certain amount of time. Once a new potential goal point is detected the subsequent Expectation Maximization like algorithm computes in the Expectation step the responsibilities of each goal for a new potential goal point $\boldsymbol{p}_i$. This is the probability of the point belonging to an existing mixture component

$$p(\boldsymbol{g}_k|\boldsymbol{p}_i) = \frac{p(\boldsymbol{p}_i|k)p(\boldsymbol{g}_k)}{p(\boldsymbol{p}_i)} = \frac{\alpha_k \, \mathcal{N}\big(\boldsymbol{p}_i \,|\, \boldsymbol{\mu}_k^g, \boldsymbol{\Sigma}_k^g\big)}{\sum_{j=1}^{K} \alpha_j \, \mathcal{N}\big(\boldsymbol{p}_i \,|\, \boldsymbol{\mu}_j^g, \boldsymbol{\Sigma}_j^g\big)}.$$

These responsibilities are then used to update the existing models and their parameters in the Maximization step:

$$\begin{aligned}
s_k &= s_k + p(g_k|\boldsymbol{p}_i), \quad v_k = \frac{p(g_k|\boldsymbol{p}_i)}{s_k}, \\
\boldsymbol{\mu}_k^g &= \boldsymbol{\mu}_k^g + v_k(\boldsymbol{p}_i - \boldsymbol{\mu}_k^g), \\
\boldsymbol{\Sigma}_k^g &= (1 - v_k)\boldsymbol{C}_k + v_k(\boldsymbol{p}_i - \boldsymbol{\mu}_k^g)(\boldsymbol{p}_i - \boldsymbol{\mu}_k)^\mathsf{T} \\
&\quad - (\tilde{v}_k - v_k)(\boldsymbol{\mu}_k^g - \boldsymbol{\mu}_k^{\text{g,old}})(\boldsymbol{\mu}_k - \boldsymbol{\mu}_k^{\text{g,old}})^\mathsf{T},
\end{aligned}$$

where s_k can be interpreted as a measure for the amount of data the component already modeled well, and v_k is an update weight. If all likelihoods $p(\boldsymbol{p}_i|k)$ are below a threshold P_{new} a new component is initialized according to

$$\boldsymbol{\mu}_{k+1} = \boldsymbol{p}_i, \qquad \boldsymbol{\Sigma}_{k+1} = \boldsymbol{\Sigma}_{init}, \qquad s_{k+1} = 1.0 \tag{12}$$

We additionally check the goals for minimal support to regard outliers and delete mixture components if they did not reach a threshold $s_k^{\min}$ after a certain lifetime.

The GMM is subsequently used by the belief tracker to track activation of goals and predict human trajectories.

2) Belief Tracker: Similar to the approach of goal directed motion prediction in [26] we introduce a probabilistic model to track the current goal of human motions. Based on a given sequence of observed human wrist positions $\boldsymbol{o}_t = (x_t^h, y_t^h, z_t^h)$ we can update our belief over goals of the human $b_t(\boldsymbol{g}_k)$, this is the belief towards which goal the human is currently reaching to. For this, we use Bayes Theorem to compute the updated belief over goals

$$b_{t+1}(\boldsymbol{g}_k) = p(\boldsymbol{g}|\boldsymbol{o}_t, \boldsymbol{b}_t) = \frac{p(\boldsymbol{o}_t|\boldsymbol{g}_k, b_t)b_t(\boldsymbol{g}_k)}{\sum_j p(\boldsymbol{o}_t|\boldsymbol{g}_j, b_t)b_t(\boldsymbol{g}_j)}, \tag{13}$$

where we compute $p(\boldsymbol{o}_t|\boldsymbol{g}_k, b_t)$ by assuming noisy goal directed movements of the human as also proposed in [26]

$$\begin{aligned}
p(\boldsymbol{o}_t|\boldsymbol{g}_k, b_t) &= \mathcal{N}(\boldsymbol{o}_t|\hat{\boldsymbol{o}}_k, \boldsymbol{I}\sigma_k), \text{ with} \\
\hat{\boldsymbol{o}}_k &= \boldsymbol{o}_{t-1} + \frac{\boldsymbol{g}_k - \boldsymbol{o}_{t-1}}{|\boldsymbol{g}_k - \boldsymbol{o}_{t-1}|} v_h \Delta t,
\end{aligned} \tag{14}$$

where $\boldsymbol{I}$ is the identity matrix, σ_k denotes noise along the trajectory towards a goal, v_h denotes the current estimated human velocity and $|\cdot|$ denotes the Euclidean norm.

Additionally, we learn the transition probabilities of a goal given a sequence of prior goals $\mathcal{G}$ from the observations

$$p(\boldsymbol{g}_k|\mathcal{G}) = \frac{\#\boldsymbol{g}_k|\mathcal{G}}{\sum_j \#\boldsymbol{g}_j|\mathcal{G}}, \tag{15}$$

where $\#\boldsymbol{g}_k|\mathcal{G}$ denotes the number of occurrences of goal k given the sequence of goals $\mathcal{G}$. Since the robot's behavior may influence the transition probabilities of the human between goals, so that it can change compared to human task execution without a robot, we propose to update these probabilities online using exponential decay for a new occurrence of goal k given the history of goals G

$$\begin{aligned}
p'(\boldsymbol{g}_k|\mathcal{G}) &= p(\boldsymbol{g}_k|\mathcal{G})(1 - \beta) + \beta \\
p'(\boldsymbol{g}_j|\mathcal{G}) &= p(\boldsymbol{g}_j|\mathcal{G})(1 - \beta) \quad \forall \quad j \neq k,
\end{aligned} \tag{16}$$

where $\beta \leq 1$ denotes the decay factor.

We represent the predicted distribution over human trajectories with M particles, where each of these particles is initialized with a goal sampled according to $p(\boldsymbol{g})$. The particle is propagated S time steps into the future towards this goal according to the probabilistic motion model in Equation (14), and in case it reaches this goal a new goal is sampled according to the transition probabilities. The resulting vector of predictions can then be used as an obstacle vector for intention aware online adaptation of ProMPs as introduced in Section III-B and III-C.

IV. Experimental Evaluation

In this section, we introduce the experimental setup and present results from evaluations with non-expert users.

A. Experimental Setup

We evaluate our proposed methods on a pick and place task in a shared workspace as shown in Figure 5(a) with 25 non-expert subjects. The task of the subjects (seated at A) is to assemble parts collected from D and E. The assembly area is at B and assembled parts should be delivered to C. The order in which the human takes D and E can be chosen freely and the subjects' motions are tracked via motion capture (G). The robot delivers parts from F to E, refilling the parts at E, for which two task space ProMPs (from F to E and from E to F) were learned from kinesthetic teaching as shown in the upper row of Figure 1. During spatial deformation we kept the orientation fixed. The demonstrations did also include trajectories that avoid potential positions of the human in the robot's workspace. After a task familiarization phase each subject performed the task under 4 different conditions (modes). In the first mode the human executed 10 repetitions of the assembly task without the robot moving. From this data, as shown in Figure 5(b), the initial motion model including motion goals and transition

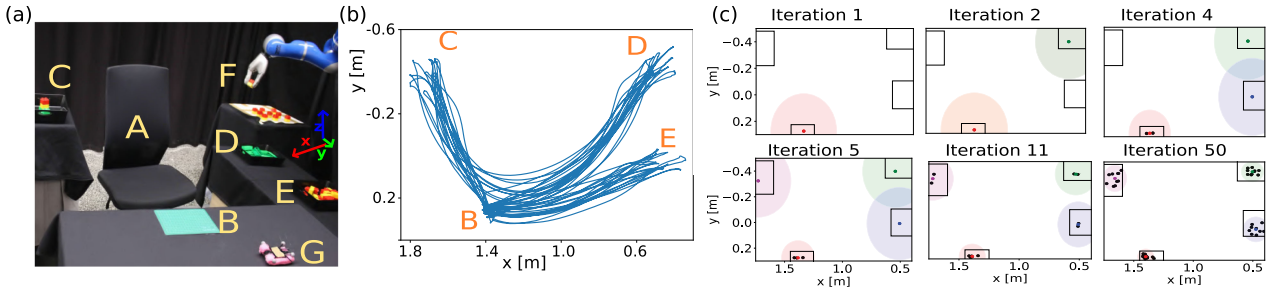

Fig. 5. (a) We evaluate the proposed approaches for intention aware online adaptation of ProMPs on a pick and place task. The human (A) assembles parts from D and E in area B and delivers them to C, while the robot refills the parts in E from F. (b) First we record motion data from the human wrist position while the robot is not moving. (c) We incrementally learn a GMM over motion goals using zero velocity points as goal candidates.

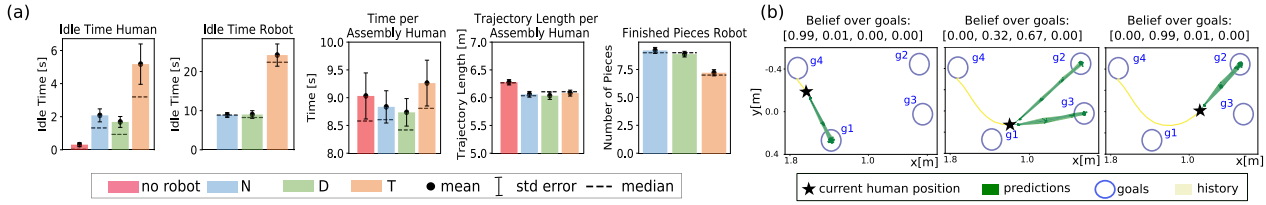

Fig. 6. (a) During the user study, we recorded and evaluated motion data from the subjects and the robot for the different adaptation modes, namely no reaction (N), spatial deformation (D) and temporal scaling (T). (b) Using a probabilistic goal directed motion model, that was learned from observation, the belief over the goals and the predictions (green) change given an observed human trajectory (yellow) and the current position (black star).

TABLE I
ACCURACY OF THE GOAL TRACKER

	Average error of learned goals [cm]
Goal 1	4.3 ± 1.6
Goal 2	4.2 ± 1.4
Goal 3	3.9 ± 1.3
Goal 4	3.8 ± 1.5

probabilities between goals was learned. In the next three modes the human performed 15 repetitions of the assembly task while the robot moved in three different ways that we will refer to as N (no adaptation, Figure 1 second row), D (spatial deformation, Figure 1 third row) and T (temporal scaling, Figure 1 last row). We recorded human and robot trajectories and additionally the subjects answered questionnaires after each experiment and three questions comparing the different adaptation modes at the end of all experiments.

B. Learning Motion Goals

When the human performed the task without the robot we recorded the wrist position of the subjects to learn motion goals and transition probabilities and average stay durations at the goals. Figure 5(c) shows how a GMM is build incrementally for the motion goals. We compare the mean of the learned goals for all subjects with the measured positions of the goals. Table I shows that for all subjects the remaining error is below 5 cm. This error can be caused due to individual placements of the motion capture markers on the subjects' hands and different distributions of the parts in the boxes. The learned motion goals were subsequently used for trajectory predictions as shown in Figure 6(b).

C. Intention Aware Online Adaptation of ProMPs

We evaluated human response to three different robot adaptation behaviors, namely no adaptation of the ProMPs (mode N), online spatial deformation (mode D) and temporal scaling (mode T), both according to predicted human trajectories. We randomized the order of the modes and the subjects were not told how or if the robot would respond to them. During the experiments, we recorded trajectories of the human and the robot and additionally, the humans answered a questionnaire after each individual mode. The questionnaire consisted of five questions:

Q1: "The robot adapted its movements to me",
Q2: "I felt disturbed by the movements of the robot",
Q3: "The behavior of the robot was predictable for me",
Q4: "I felt uncomfortable due to the robot's movements",
Q5: "I trusted the robot not to hurt me".

For all questions, we evaluated approval on a 5 point Likert scale. The subjects also took notes on how they would describe the robot behavior after each mode. Additionally, the subjects were asked to answer three comparison questions, in the end, on which of the modes made them feel 1) most uncomfortable, 2) most safe and 3) least disturbed.

We evaluated idle times of the human and robot, average trajectory length and time per assembly of the human, and number of finished pieces of the robot. Figure 6(a) shows the results. After removing one outlier subject, who tested the robot extensively such that idle times deviated from the other subjects, we ran non-parametric ANOVA with Kruskal-Wallis and a posthoc Conovers test, since the data showed no normal distribution according to the Shapiro-Wilk test. We chose a significance level of $\alpha = 0.05$ which is common in the literature [11]. The tests show that the human idle time was significantly higher when the robot was present compared to the no robot

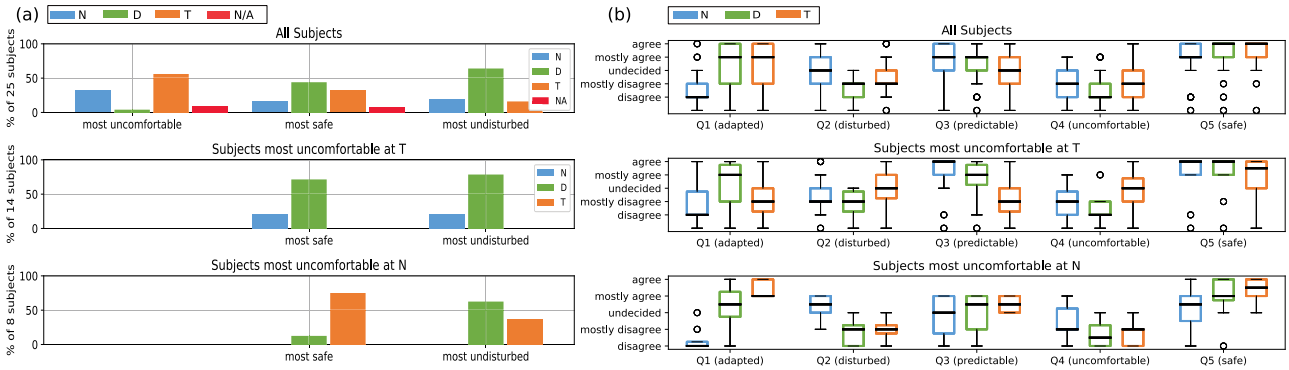

Fig. 7. (a) The subjects answered comparison questions on in which mode (no reaction (N), spatial deformation (D) and temporal scaling (T)) they felt 1) most uncomfortable due to the robot's movements, 2) most safe and 3) most undisturbed. (b) The subjects additionally answered a questionnaire after each experiment mode where we evaluated 5 questions that were answered on a 5 point Likert scale. The results are visualized as box plots including the median (black horizontal line), interquartile range (box), 1.5 whiskers (fine black lines), and outliers (black circles).

mode ($p < 0.0004$). The average idle time was higher in the temporal mode than in the spatial mode and in the unreactive mode. In the experiments we noticed that it was after some time very easy for the subjects to adapt their own task rhythm to the constant rhythm of the robot in the unreactive mode. The robot idle times at the non responsive mode result from the grasping time of the hand. The total trajectory length per assembly of the human shows that in the first experiment without the robot the average length was lower in the modes where the robot was present. As for all subjects the experiment without the robot was the first experiment, this can be explained by task adaptation of the human after the first experiment. The behavior of the robot did not influence the average trajectory length. In combination with the idle times this shows that the human rather stopped and waited for a situation to clarify instead of spatially evading the robot in the experimental setting. The data shows that the number of finished pieces is significantly lower in the temporal mode ($p < 0.00002$). The human always finished 15 pieces as this marked the end of the experiment. The mean assembly time of the humans was smallest in the spatial deformation mode, however no statistical significance was found ($p = 0.96$).

Figure 7(a) shows the result of the subjective comparison of the three modes. The upper row shows that 32% of the subjects felt most uncomfortable in the unresponsive mode, 52% percent felt most uncomfortable during temporal scaling and 4% during spatial deformation. 8% reported that they never felt uncomfortable. When looking at these two groups individually it shows that the ones that felt uncomfortable with the unresponsive robot in particular felt safe at temporal scaling and the ones that felt most uncomfortable with temporal scaling felt most safe during spatial deformation. In general, subjects reported that they felt more undisturbed at spatial deformation. In the experiment notes subjects reported that during the temporal scaling mode they felt the robot's productivity decreased when the robot needed to stop because of them and this "ineffective task execution" made them feel uncomfortable. Additionally, subjects reported the robot stopping in too close distance to a goal disturbed them. However, another group of subjects reported that they found the motions of the robot to be very controlled, safe, and reactive when it was in temporal scaling mode. Figure 7(b) shows the subjective answers to the questions on the single modes. We ran a non parametric ANOVA using Kruskal Wallis test and posthoc Conover's test on this data. The test showed that all subjects found the robot significantly more adaptive in temporal scaling and spatial deformation mode compared to no reaction ($p = 0.0002$). Subjects also felt significantly less disturbed in spatial deformation mode compared to no reaction ($p = 0.032$) and they found the robot significantly less predictable in temporal scaling mode compared to no reaction ($p = 0.012$). When only considering the subjects that felt most uncomfortable at temporal scaling mode the subjects found the robot significantly more unpredictable in temporal mode than in spatial or non reactive ($p < 0.048$), and felt significantly more uncomfortable in temporal scaling than in spatial deformation mode ($p = 0.02$). In average the robot was perceived less adaptive in the temporal mode. On the other hand subjects that felt most uncomfortable in the non reactive mode found in average the temporal mode more adaptive than the spatial deformation mode. In terms of comfort and safety no statistical significance can be found between the modes when looking at data of all subjects.

The results of this user study already provide valuable insights on human reactions to online adaptation of ProMPs. However, for future studies a wide variety of experimental settings should be evaluated in order to get more generalizable insights. In particular, also different slowing down and speeding up behaviors in the temporal scaling mode should be compared, as in the experiments we noticed that to abrupt slowing down or speeding up may irritate the users.

V. Conclusion

We presented two novel approaches for intention aware online adaptation of ProMPs, namely online spatial deformation and temporal scaling. We evaluated both approaches on a pick and place task with 25 non-expert subjects where we analyzed motion data as well as questionnaires on subjective comfort level and perceived safety. The subjects reported a higher level of perceived safety and felt less disturbed during intention aware adaptation, in particular during spatial deformation. The results indicate that human responses to different kinds of robot behavior do not necessarily generalize across all subjects. In particular, temporal scaling was perceived by one group of subjects as disturbing and unpredictable but as safe and predictable by another group.

Subjects in general felt uncomfortable and got annoyed if they found the robot behavior unpredictable or if they did not

understand why a certain robot response was occurring. Therefore, incorporating more communication including motion cues and/or visual feedback should be investigated. Additionally, the experiments revealed that different subjects preferred different robot behaviors. For future work, we plan to investigate how to derive a hierarchical model from these insights that would online classify user types and adapt robot behavior accordingly. Moreover, combinations of spatial and temporal ProMP adaptation could be investigated. Extending the prediction model to incorporate more complex human trajectory behavior and additional intention cues such as gaze direction and body posture is another line for future research.

REFERENCES

[1] B. Alenljung, J. Lindblom, R. Andreasson, and T. Ziemke, "User experience in social human-robot interaction," *Int. J. Ambient Comput. Intell.*, vol. 8, no. 2, pp. 12–31, 2017.

[2] T. Osa *et al.*, "An algorithmic perspective on imitation learning," in *Foundations and Trends in Robotics*, vol. 7, no. 1–2, pp. 1–179, 2018.

[3] A. J. Ijspeert, J. Nakanishi, H. Hoffmann, P. Pastor, and S. Schaal, "Dynamical movement primitives: Learning attractor models for motor behaviors," *Neural Comput.*, vol. 25, no. 2, pp. 328–373, 2013.

[4] S. Calinon, F. Guenter, and A. Billard, "On learning, representing, and generalizing a task in a humanoid robot," *IEEE Trans. Syst., Man, Cybernet.*, vol. 37, no. 2, pp. 286–298, Apr. 2007.

[5] A. Paraschos, C. Daniel, J. Peters, and G. Neumann, "Using probabilistic movement primitives in robotics," *Auton. Robots*, vol. 42, no. 3, pp. 529–551, 2018.

[6] G. J. Maeda, G. Neumann, M. Ewerton, R. Lioutikov, O. Kroemer, and J. Peters, "Probabilistic movement primitives for coordination of multiple human–robot collaborative tasks," *Auton. Robots*, vol. 41, no. 3, pp. 593–612, 2017.

[7] D. Koert, G. Maeda, R. Lioutikov, G. Neumann, and J. Peters, "Demonstration based trajectory optimization for generalizable robot motions," in *Proc, IEEE-RAS 16th Int. Conf. Humanoid Robots Humanoids*, 2016, pp. 515–522.

[8] A. Colomé and C. Torras, "Demonstration-free contextualized probabilistic movement primitives, further enhanced with obstacle avoidance," in *Proc. IEEE/RSJ Int. Conf. Intell. Robots Syst.*, 2017, pp. 3190–3195.

[9] M. Huber, Y.-H. Su, M. Krüger, K. Faschian, S. Glasauer, and J. Hermsdörfer, "Adjustments of speed and path when avoiding collisions with another pedestrian," *PLoS One*, vol. 9, no. 2, 2014, Art. no. e89589.

[10] I. Karamouzas and M. Overmars, "Simulating human collision avoidance using a velocity-based approach," in *Proc. 7th Workshop Virtual Reality Interact. Phys. Simul.*, 2010, pp. 125–134.

[11] P. A. Lasota and J. A. Shah, "Analyzing the effects of human-aware motion planning on close-proximity human–robot collaboration," *Human Factors*, vol. 57, no. 1, pp. 21–33, 2015.

[12] T. Arai, R. Kato, and M. Fujita, "Assessment of operator stress induced by robot collaboration in assembly," *CIRP Ann.*, vol. 59, no. 1, pp. 5–8, 2010.

[13] A. D. Dragan, K. C. Lee, and S. S. Srinivasa, "Legibility and predictability of robot motion," in *Proc. 8th ACM/IEEE Int. Conf. Human-Robot Interact*, 2013, pp. 301–308.

[14] M. Vasic and A. Billard, "Safety issues in human-robot interactions," in *Proc. IEEE Int. Conf. Robot. Autom.*, 2013, pp. 197–204.

[15] D. Kulić and E. A. Croft, "Safe planning for human-robot interaction," *J. Robot. Syst.*, vol. 22, no. 7, pp. 383–396, 2005.

[16] M. Koppenborg, P. Nickel, B. Naber, A. Lungfiel, and M. Huelke, "Effects of movement speed and predictability in human–robot collaboration," *Human Factors Ergonom. Manuf. Service Industries*, vol. 27, no. 4, pp. 197–209, 2017.

[17] C. Morato, K. N. Kaipa, B. Zhao, and S. K. Gupta, "Toward safe human robot collaboration by using multiple kinects based real-time human tracking," *J. Comput. Inf. Sci. Eng.*, vol. 14, no. 1, 2014, Art. no. 011006.

[18] J. Mainprice, R. Hayne, and D. Berenson, "Predicting human reaching motion in collaborative tasks using inverse optimal control and iterative re-planning," in *Proc. IEEE Int. Conf. Robot. Autom.*, 2015, pp. 885–892.

[19] R. Hayne, R. Luo, and D. Berenson, "Considering avoidance and consistency in motion planning for human-robot manipulation in a shared workspace," in *Proc. IEEE Int. Conf. Robot. Autom.*, 2016, pp. 3948–3954.

[20] D. P. Losey and M. K. OMalley, "Trajectory deformations from physical human–robot interaction," *IEEE Trans. Robot.*, vol. 34, no. 1, pp. 126–138, Feb. 2018.

[21] B. Busch, G. Maeda, Y. Mollard, M. Demangeat, and M. Lopes, "Postural optimization for an ergonomic human-robot interaction," in *Proc. IEEE/RSJ Int. Conf. Intell. Robots Syst.*, 2017, pp. 2778–2785.

[22] E. A. Sisbot and R. Alami, "A human-aware manipulation planner," *IEEE Trans. Robot.*, vol. 28, no. 5, pp. 1045–1057, Oct. 2012.

[23] J. Mainprice and D. Berenson, "Human-robot collaborative manipulation planning using early prediction of human motion," in *Proc. IEEE/ RSJ Int. Conf. Intell. Robots Syst.*, 2013, pp. 299–306.

[24] E. A. Sisbot, L. F. Marin-Urias, X. Broquere, D. Sidobre, and R. Alami, "Synthesizing robot motions adapted to human presence," *Int. J. Social Robot.*, vol. 2, no. 3, pp. 329–343, 2010.

[25] F. G. Lopez, J. Abbenseth, C. Henkel, and S. Dörr, "A predictive online path planning and optimization approach for cooperative mobile service robot navigation in industrial applications," in *Proc. Euro. Conf. Mobile Robots*, 2017, pp. 1–6.

[26] H. Bai, S. Cai, N. Ye, D. Hsu, and W. S. Lee, "Intention-aware online POMDP planning for autonomous driving in a crowd," in *Proc. IEEE Int. Conf. Robot. Autom.*, 2015, pp. 454–460.

[27] P. Trautman and A. Krause, "Unfreezing the robot: Navigation in dense, interacting crowds," in *Proc. IEEE/RSJ Int. Conf. Intell. Robots Syst.*, 2010, pp. 797–803.

[28] T. Kruse, P. Basili, S. Glasauer, and A. Kirsch, "Legible robot navigation in the proximity of moving humans," in *Proc. IEEE Workshop Adv. Robot. Social Impacts*, 2012, pp. 83–88.

[29] T. Ikeda, Y. Chigodo, D. Rea, F. Zanlungo, M. Shiomi, and T. Kanda, "Modeling and prediction of pedestrian behavior based on the sub-goal concept," *Robotics*, vol. 10, pp. 137–144, 2013.

[30] H. C. Ravichandar and A. Dani, "Human intention inference through interacting multiple model filtering," in *Proc. IEEE Int. Conf. Multisensor Fusion Integration for Intell. Syst.*, 2015, pp. 220–225.

[31] R. Luo, R. Hayne, and D. Berenson, "Unsupervised early prediction of human reaching for human–robot collaboration in shared workspaces," *Auton. Robots*, vol. 42, no. 3, pp. 631–648, 2018.

[32] O. Dermy, A. Paraschos, M. Ewerton, J. Peters, F. Charpillet, and S. Ivaldi, "Prediction of intention during interaction with iCub with probabilistic movement primitives," *Frontiers Robot. AI*, vol. 4, 2017, Art. no. 45.

[33] V. V. Unhelkar *et al.*, "Human-aware robotic assistant for collaborative assembly: Integrating human motion prediction with planning in time," *IEEE Robot. Automat. Lett.*, vol. 3, no. 3, pp. 2394–2401, Jul. 2018.

[34] D.-H. Park, H. Hoffmann, P. Pastor, and S. Schaal, "Movement reproduction and obstacle avoidance with dynamic movement primitives and potential fields," in *Proc. 8th IEEE-RAS Int. Conf. Humanoid Robots*, 2008, pp. 91–98.

[35] H. Hoffmann, P. Pastor, D.-H. Park, and S. Schaal, "Biologically-inspired dynamical systems for movement generation: Automatic real-time goal adaptation and obstacle avoidance," in *Proc. IEEE Int. Conf. Robot. Autom.*, 2009, pp. 2587–2592.

[36] S. M. Khansari-Zadeh and A. Billard, "A dynamical system approach to realtime obstacle avoidance," *Auton. Robots*, vol. 32, no. 4, pp. 433–454, 2012.

[37] M. Saveriano, F. Hirt, and D. Lee, "Human-aware motion reshaping using dynamical systems," *Pattern Recognit. Lett.*, vol. 99, pp. 96–104, 2017.

[38] D. Pavlichenko and S. Behnke, "Efficient stochastic multicriteria arm trajectory optimization," in *Proc. IEEE/RSJ Int. Conf. Intell. Robots Syst.*, 2017, pp. 4018–4025.

[39] P. M. Engel and M. R. Heinen, "Incremental learning of multivariate gaussian mixture models," in *Proc. Brazilian Symp. Artif. Intell.*, 2010, pp. 82–91.